

Supporting information

Synergetic effect between spin crossover and luminescence in complex $[\text{Fe}(\text{bpp})_2][\text{BF}_4]_2$ ($\text{bpp}=2,6\text{-bis(pyrazol-1-yl)pyridine}$)

Yang Jiao,¹ Jianping Zhu,¹ Yan Guo, Weijiang He* and Zijian Guo*

State Key Laboratory of Coordination Chemistry, Coordination Chemistry Institute, School of Chemistry and Chemical Engineering, Nanjing University, Nanjing, P. R. China.

¹ The two authors contributed equally to this work.

E-mail: hewej69@nju.edu.cn, zguo@nju.edu.cn

Table of Contents

1. Fig. S1 ^1H NMR spectrum of bpp in CDCl_3	S2
2. Fig. S2 ^{13}C NMR spectrum of bpp in CDCl_3	S2
3. Fig. S3 Molecular structure of $[\text{Fe}(\text{bpp})_2][\text{BF}_4]_2$	S3
4. Fig. S4 Plot of $\chi_M T$ versus T for $[\text{Fe}(\text{bpp})_2][\text{BF}_4]_2$	S3
5. Fig. S5 Reflection UV-vis spectrum of solid $[\text{Fe}(\text{bpp})_2][\text{BF}_4]_2$ at 298 K.....	S4
6. Fig. S6 UV-vis absorbance spectrum of $[\text{Fe}(\text{bpp})_2][\text{BF}_4]_2$ in DMF.....	S4
7. Fig. S7 Photo of solid $[\text{Fe}(\text{bpp})_2][\text{BF}_4]_2$ at different temperatures	S5
8. Fig. S8 Luminescence spectra of bpp and $[\text{Fe}(\text{bpp})_2][\text{BF}_4]_2$ in DMF	S5
9. Fig. S9 Hole/electron distribution patterns of other transitions in $[\text{Fe}(\text{bpp})_2][\text{BF}_4]_2$	S6
10. Fig. S10 Scheme of the frontier MOs of HS state of complex $[\text{Fe}(\text{bpp})_2][\text{BF}_4]_2$	S7
11. Note S1 Identification of other MLCT transitions.....	S8
12. Table S1 Crystal data and structure refinement for $[\text{Fe}(\text{bpp})_2][\text{BF}_4]_2$	S9
13. Table S2 Selected bond lengths (\AA) and angles ($^\circ$) for $[\text{Fe}(\text{bpp})_2][\text{BF}_4]_2$	S10
14. Table S3 Calculated allowed transitions of complex $[\text{Fe}(\text{bpp})_2][\text{BF}_4]_2$	S11
15. Table S4 Transition MOs for the lowest allowed transitions of complex $[\text{Fe}(\text{bpp})_2][\text{BF}_4]_2$	S11
16. Table S5 Transition MOs for primary transitions in $[\text{Fe}(\text{bpp})_2][\text{BF}_4]_2$ LS states.....	S12
17. Table S6 Transition MOs for primary transitions in $[\text{Fe}(\text{bpp})_2][\text{BF}_4]_2$ HS states.....	S13
18. Table S7 Occupancy and energy of Fe 3-d NAOs.....	S14
19. Table S8 Orbital composition of MO-113A in HS state.....	S15
20. Table S9 Orbital composition of MO-120B in HS state.....	S15
21. Table S10 Orbital composition of MO-118 in LS state.....	S16
22. Table S11 Orbital composition of MO-119 in LS state.....	S17
23. Table S12 Orbital composition of MO-123 in LS state.....	S18
24. Table S13 Orbital composition of MO-124 in LS state.....	S19
25. Table S14 Orbital composition of MO-126 in LS state.....	S20
26. Table S15 Orbital composition of MO-129 in LS state.....	S21
27. Table S16 Orbital composition of MO-122A in HS state.....	S22
28. Table S17 Orbital composition of MO-123A in HS state.....	S23
29. Table S18 Orbital composition of MO-125A in HS state.....	S24
30. Table S19 Orbital composition of MO-126A in HS state.....	S25
31. Table S20 Orbital composition of MO-127A in HS state.....	S26
32. Table S21 Orbital composition of MO-128A in HS state.....	S27
33. Table S22 Orbital composition of MO-117B in HS state.....	S28
34. Table S23 Orbital composition of MO-118B in HS state.....	S29
35. Table S24 Orbital composition of MO-119B in HS state.....	S30
36. Table S25 Orbital composition of MO-121B in HS state.....	S31
37. Table S26 Orbital composition of MO-123B in HS state.....	S32
38. Table S27 Orbital composition of MO-124B in HS state.....	S33
39. Table S28 Orbital composition of MO-126B in HS state.....	S34

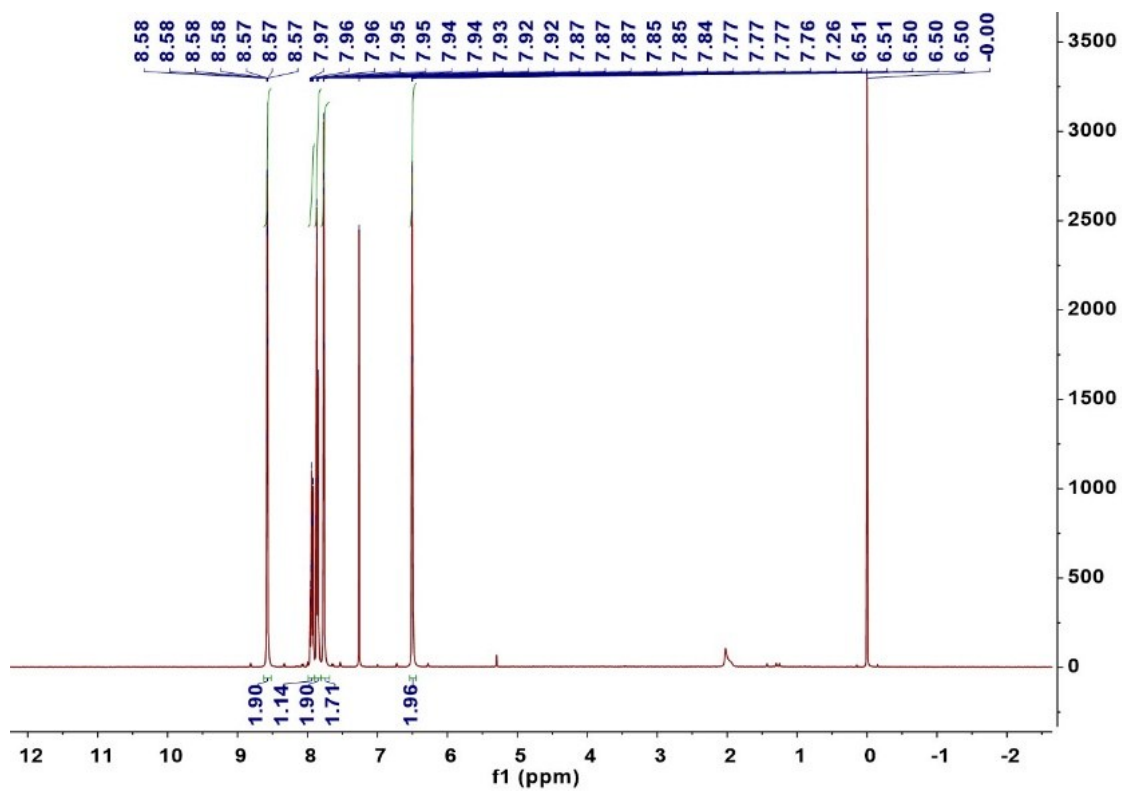


Fig. S1 ^1H NMR spectrum of bpp in CDCl_3 .

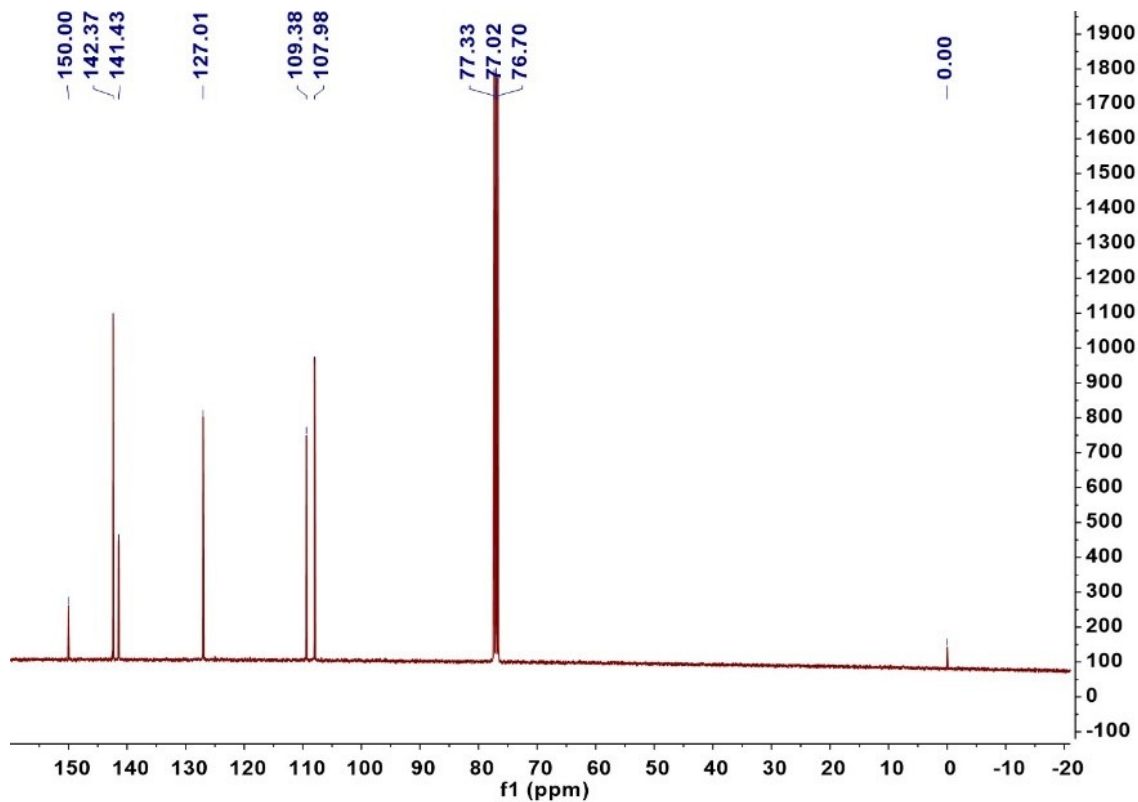


Fig. S2 ^{13}C NMR spectrum of bpp in CDCl_3 .

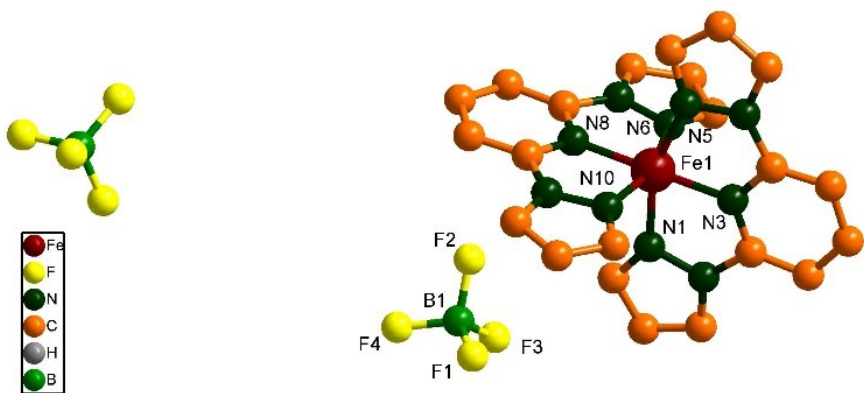


Fig. S3 Molecular structure of complex $[\text{Fe}(\text{bpp})_2]\text{[BF}_4\text{]}_2$ (all the hydrogen atoms are omitted for clarity).

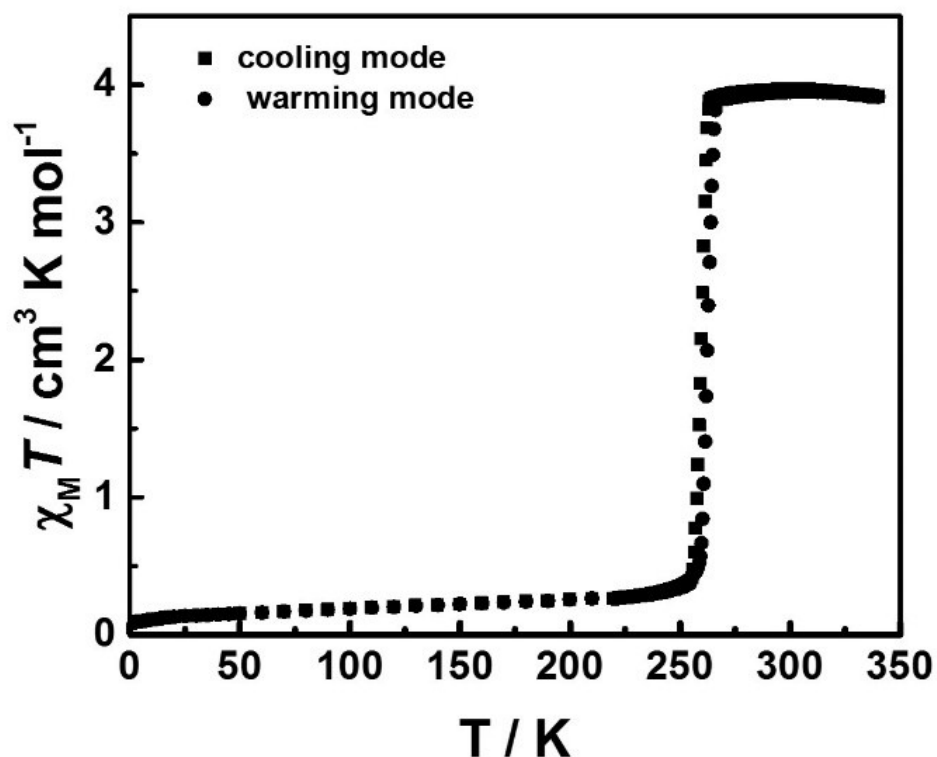


Fig. S4 Plot of $\chi_M T$ versus T for complex $[\text{Fe}(\text{bpp})_2]\text{[BF}_4\text{]}_2$ in cooling and warming modes.

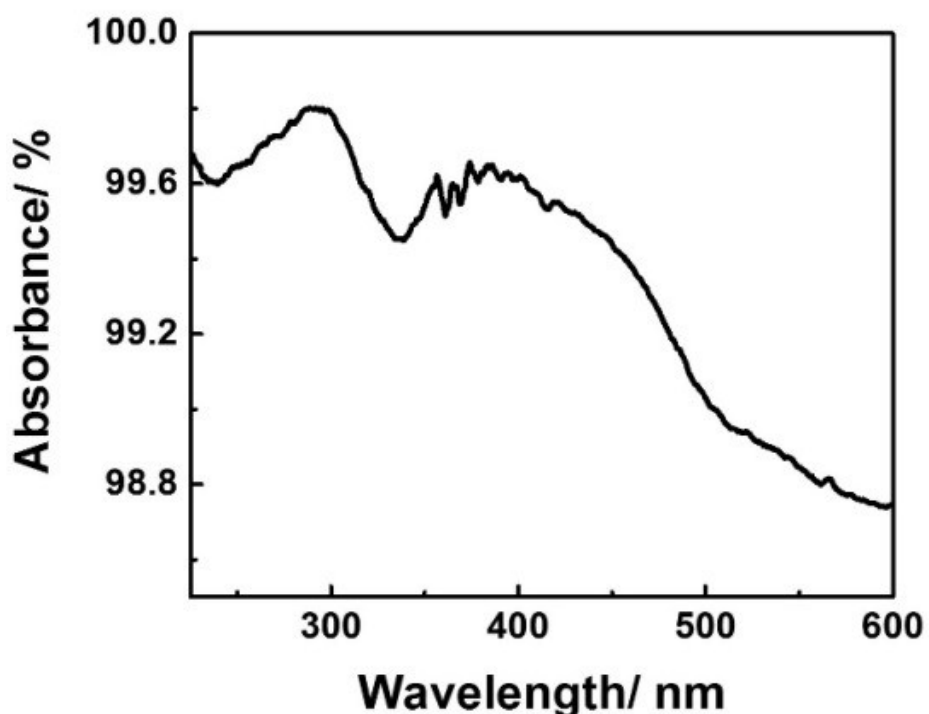


Fig. S5 Reflection UV-vis spectrum of solid $[\text{Fe}(\text{bpp})_2]\text{[BF}_4\text{]}_2$ at room temperature (298 K).

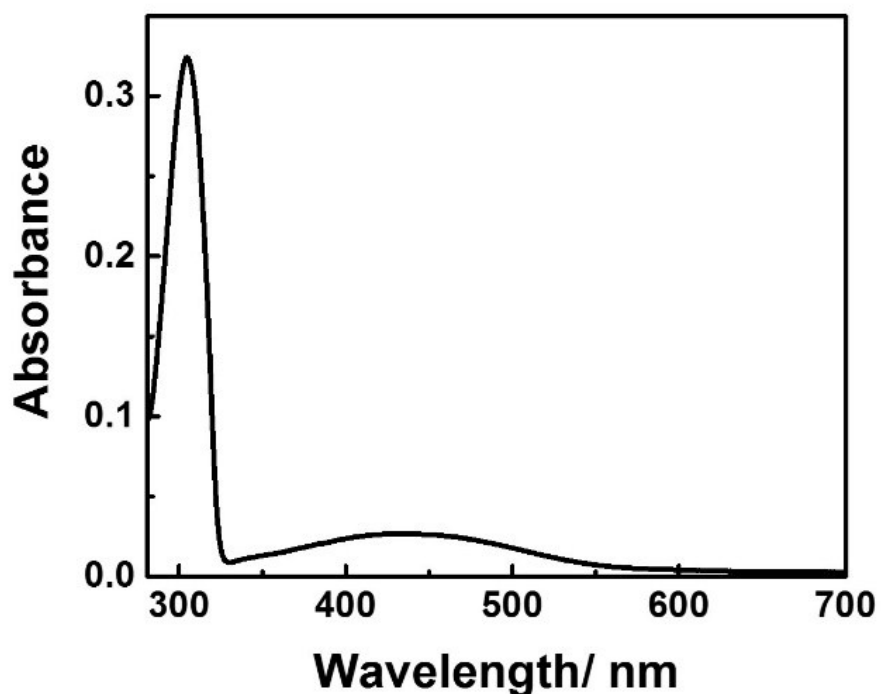


Fig. S6 UV-vis absorption spectrum of $[\text{Fe}(\text{bpp})_2]\text{[BF}_4\text{]}_2$ ($10\mu\text{M}$) in DMF determined at room temperature (298 K).

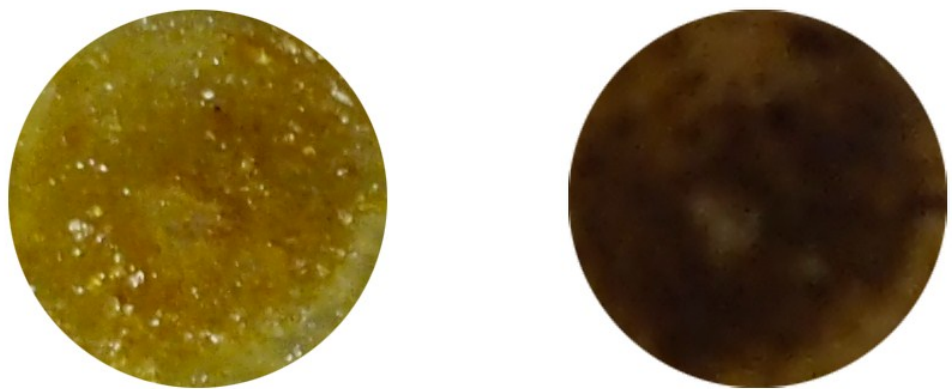


Fig. S7 Photographs of solid $[\text{Fe}(\text{bpp})_2]\text{[BF}_4\text{]}_2$ at room temperature (left) and upon cooling with liquid nitrogen (right).

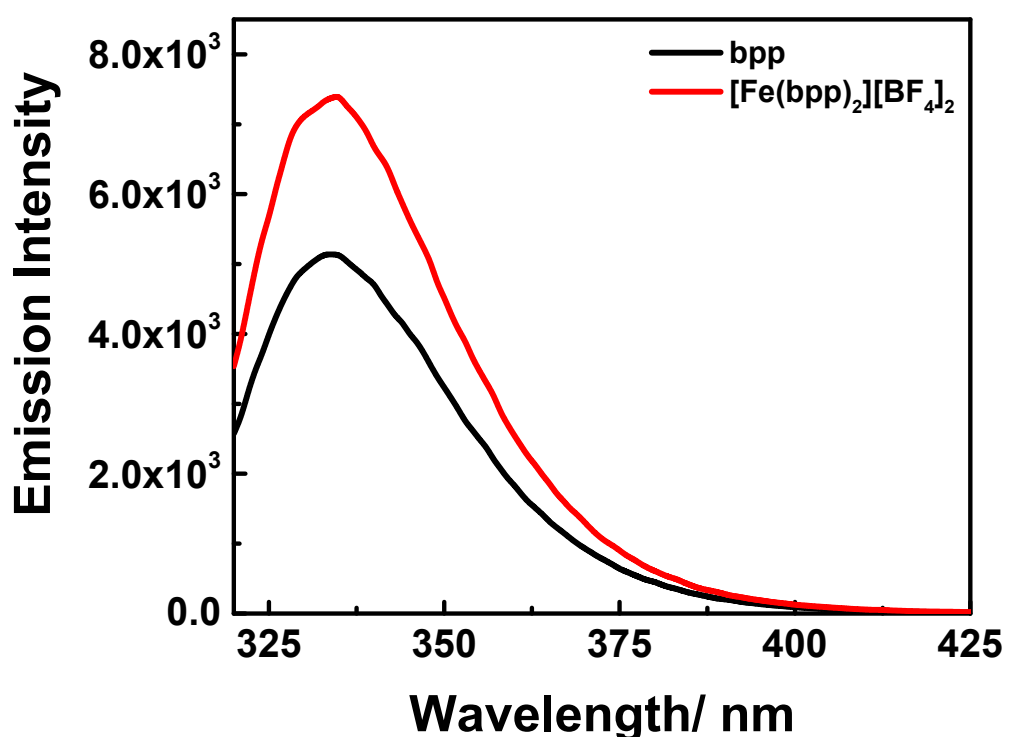
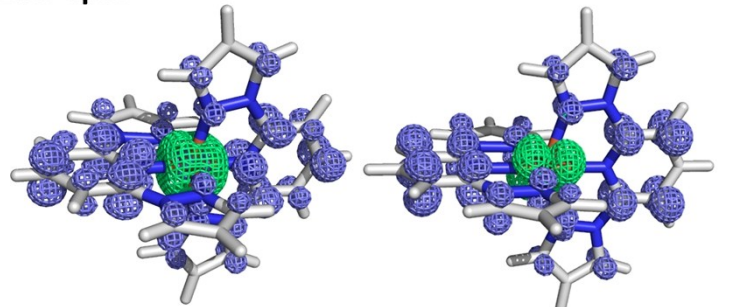


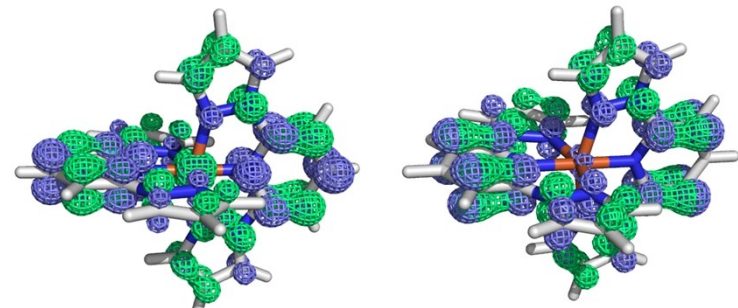
Fig. S8 Luminescence spectra of bpp and $[\text{Fe}(\text{bpp})_2]\text{[BF}_4\text{]}_2$ (10 μM) in DMF at ambient temperature.

Low Spin



Transition 11

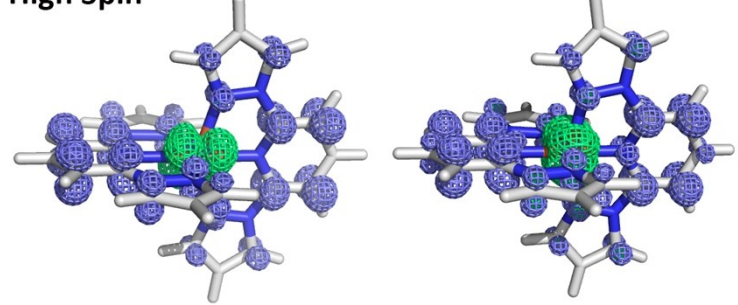
Transition 13



Transition 19

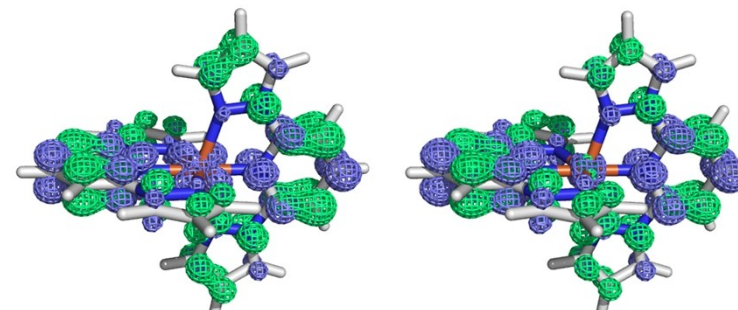
Transition 24

High Spin



Transition 7

Transition 8



Transition 19

Transition 28

Fig. S9 Hole (green mesh) and electron (blue mesh) distributions for LS transitions 11, 13, 19, 24, and HS transitions 7, 8, 19, 28 of complex $[\text{Fe}(\text{bpp})_2][\text{BF}_4]_2$.

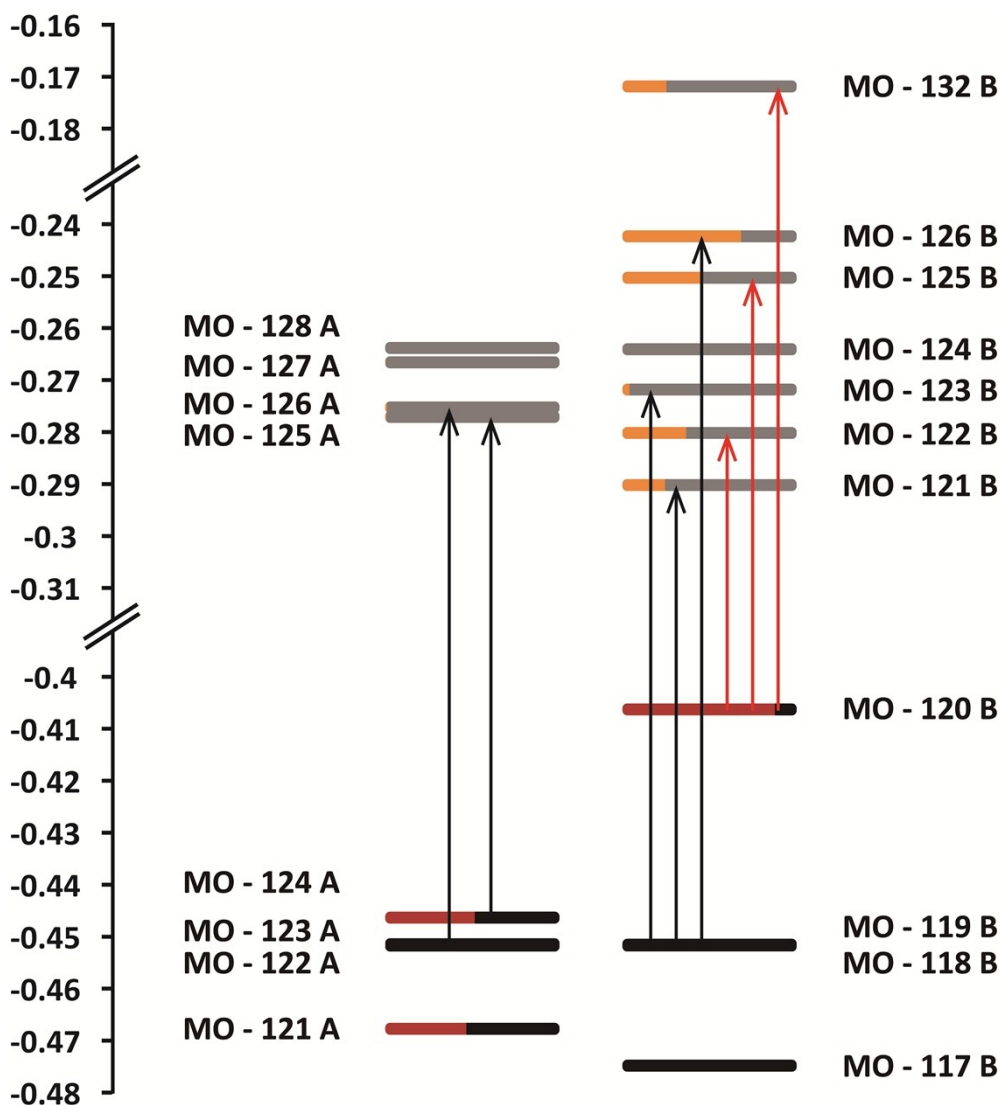


Fig. S10 Scheme of the frontier MOs of HS state for $[\text{Fe}(\text{bpp})_2][\text{BF}_4]_2$. Red and Black bars represent the occupied orbitals, orange and grey bars represent the unoccupied orbitals. The length of red and orange parts in all the bars is proportional to the Fe contribution. Transition 7 shown as red arrow, transition 19 shown as black arrow.

NOTE S1 Identification of other MLCT transition.

According to Table S3, electrons for transitions 11 and 13 of LS state transit from MO-120, 121, and 122, which are composed mainly by Fe atom (Table 3), to MO-123, 124, and 126, which are contributed the ligand (Table S10-S12). The transitions with even higher energy are in a different style. For example, transition 19 mainly contributed by orbital pairs originated by ligand. The orbital pairs MO120 to MO125 and MO122 to MO129, which are attributed to metal to ligand transition, have relatively low correlation coefficients (the absolute values are about 0.11, Table S3). This means transition 19 is mainly contributed by intra-ligand. Transition 24 is composed by MO-118 to 126 and MO-119 to 125, little composition of Fe is contained. The orbital components for the ligand based orbitals can be found in Table S8 to S13.

The situation of HS state is more complicated that most transitions contain multiple orbital pairs rather than one or two pairs of the predominant role. Moreover, the percentage of Fe NAO in the certain MO is not as high as in LS state. Consequently, the transitions in HS state are not easily to be assigned to pure type. Nevertheless, the disparity of MLCT proportion can still be evaluated. The frontier MOs scheme (Fig. S10) shows the different pattern between transition 7 and transition 19. In the former, the electrons leave the Fe dominated MO 120B for the MOs with less Fe contributions, namely, MO 122B, MO 125B, and MO 132B, showing the explicit MLCT property. According to Table S4 and orbital components listed in Table S14 to S26, transition 8 is also contributed by MLCT, whereas the higher energy transitions are different. For example, transition 19 only has a small amount of MLCT composition (MO-124A to MO-126A with coefficient of 0.44, Table S4), and intra-ligand transitions (123A to 125A and 118B to 123B), as well as the ligand-to-metal transitions (119B to 121B and 119B to 126B) have higher contribution. Transitions 20, 24, 27, and 28 are similar to transition 19. In transition 28, the coefficient of MO pair 121A to 126A, which is attributed to MLCT, is only 0.16. The LMCT pairs 117B to 122B and 119B to 121B also exhibits low coefficients (0.11 and -0.14). Intra-ligand transitions (123A to 125A with -0.59, 118B to 123B with 0.78) are predominant.

Table S1. Crystal data and structure refinement for **[Fe(bpp)₂][BF₄]₂**.

Complex	[Fe(bpp) ₂][BF ₄] ₂
Formula	C ₂₂ H ₁₈ B ₂ F ₈ FeN ₁₀
Fw	651.93
Temp(K)	153(2)
λ (Mo Kα), Å	0.71073
Crystal system	Monoclinic
Space group	P2 ₁
a (Å)	8.4437(12)
b (Å)	8.5084(11)
c (Å)	18.348(3)
α(deg)	90
β(deg)	98.354(4)
γ(deg)	90
V (Å ³)	1304.2(3)
Z	2
F(000)	656.0
2θ range for data collection (deg)	4.488 to 55.168
Final R ₁ ^a , wR ₂ ^b	0.0475, 0.1210
Goodness-of-fit on F ²	1.167

^aR₁ = $\sum |F_o| - |F_c| / \sum |F_o|$. ^bwR₂ = $[\sum w(F_o^2 - F_c^2)^2 / \sum w(F_o^2)]^{1/2}$. w = $1/[\sigma^2(F_o) + 0.0297 P^2 + 27.5680P]$, where P = (F_o² + 2F_c²)/3.

Table S2. Selected bond lengths (\AA) and angles ($^\circ$) for $[\text{Fe}(\text{bpp})_2][\text{BF}_4]_2$.

Fe(bpp) ₂][BF ₄] ₂			
Fe(1)-N(3)	1.896(4)	Fe(1)-N(6)	1.973(5)
Fe(1)-N(1)	1.972(5)	Fe(1)-N(5)	1.979(5)
Fe(1)-N(8)	1.911(5)	Fe(1)-N(10)	1.984(5)
N(3)-Fe(1)-N(6)	98.17(19)	N(3)-Fe(1)-N(1)	80.15(19)
N(3)-Fe(1)-N(5)	79.93(19)	N(3)-Fe(1)-N(8)	178.1(2)
N(3)-Fe(1)-N(10)	101.92(19)	N(6)-Fe(1)-N(5)	92.21(19)
N(6)-Fe(1)-N(10)	159.82(18)	N(1)-Fe(1)-N(6)	90.11(19)
N(1)-Fe(1)-N(5)	160.07(19)	N(1)-Fe(1)-N(10)	91.41(19)
N(5)-Fe(1)-N(10)	93.18(19)	N(8)-Fe(1)-N(6)	80.11(19)
N(8)-Fe(1)-N(1)	98.93(19)	N(8)-Fe(1)-N(5)	100.97(19)
N(8)-Fe(1)-N(10)	79.78(19)		

Table S3. Calculated allowed transitions (oscillator strength ≥ 0.0050) for LS and HS states of complex $[\text{Fe}(\text{bpp})_2][\text{BF}_4]_2$.

	Transition energy	Wavelength	Oscillator	$\langle S^{**2} \rangle$
	Low	Spin		
Excited state 4	2.92	424.8	0.0070	0
Excited state 5	2.92	424.7	0.0069	0
Excited state 11	3.39	365.5	0.0421	0
Excited state 13	3.51	352.9	0.0877	0
Excited state 14	3.67	338.1	0.0056	0
Excited state 15	3.67	338.1	0.0056	0
Excited state 19	4.26	291.1	0.2025	0
Excited state 20	4.26	291.1	0.2027	0
Excited state 24	4.59	269.9	0.0104	0
Excited state 27	4.80	258.4	0.0776	0
	High	Spin		
Excited state 5	2.75	451.5	0.0287	7.08
Excited state 19	3.94	314.7	0.0861	6.48
Excited state 20	3.94	314.5	0.0867	6.49
Excited state 24	4.11	301.9	0.0256	6.47
Excited state 27	4.27	290.1	0.0637	6.77
Excited state 28	4.28	289.9	0.0631	7.14
Excited state 30	4.30	288.3	0.0255	6.35
Excited state 31	4.33	286.1	0.0214	6.32
Excited state 32	4.35	285.0	0.0075	6.27
Excited state 33	4.41	281.1	0.0094	6.89
Excited state 38	4.49	276.2	0.0098	6.87
Excited state 39	4.50	275.4	0.0228	6.93

Table S4 Transition MOs with coefficient's absolute value larger than 0.1 for the lowest allowed transitions in LS and HS states of complex $[\text{Fe}(\text{bpp})_2][\text{BF}_4]_2$.

	Transition MOs	Coefficient
LS transition 4	120 to 127	-0.1854
	121 to 130	-0.23411
	122 to 123	0.62982
LS transition 5	120 to 130	0.23416
	121 to 127	0.18537
	122 to 124	0.6298
HS transition 5	120B to 121B	0.7167
	120B to 126B	-0.67098

Table S5. Transition MOs with coefficient's absolute value larger than 0.1 for primary transitions in LS states of complex $[\text{Fe}(\text{bpp})_2][\text{BF}_4]_2$.

	Transition MOs	Coefficient
LS transition 11	120 to 123	0.4266
	121 to 124	0.4266
	122 to 126	-0.34981
LS transition 13	120 to 123	0.24171
	121 to 124	0.2417
	122 to 126	0.61265
LS transition 19	118 to 123	-0.12607
	118 to 124	0.38175
	119 to 123	0.51938
LS transition 20	120 to 125	-0.11282
	122 to 129	0.10609
	118 to 123	0.38316
LS transition 24	119 to 124	0.51916
	120 to 126	-0.12934
	121 to 125	-0.11286
LS transition 24	118 to 126	-0.43363
	119 to 125	0.55714

Table S6. Transition MOs with coefficient's absolute value larger than 0.1 for primary transitions in HS states of complex $[\text{Fe}(\text{bpp})_2][\text{BF}_4]_2$.

	Transition MOs	Coefficient
HS transition 7	120B to 122B	-0.65208
	120B to 125B	0.72515
	120B to 132B	0.11858
HS transition 8	120B to 124B	0.98492
	122A to 126A	0.4363
	123A to 125A	-0.48674
HS transition 19	118B to 123B	-0.21873
	119B to 121B	0.6854
	119B to 126B	0.13015
HS transition 20	122A to 125A	-0.47673
	123A to 126A	0.44571
	118B to 121B	0.68596
HS transition 24	118B to 126B	0.12932
	119B to 123B	-0.21673
	122A to 127A	0.17249
HS transition 27	123A to 128A	-0.16028
	124A to 128A	-0.10694
	118B to 122B	0.82789
HS transition 28	118B to 125B	0.32308
	119B to 124B	-0.27195
	121A to 125A	0.32156
HS transition 27	122A to 125A	-0.43129
	123A to 126A	0.10844
	118B to 121B	-0.14546
HS transition 28	119B to 123B	0.78514
	121A to 126A	0.16463
	123A to 125A	-0.58996
HS transition 28	117B to 122B	0.10767
	118B to 123B	0.73978
	119B to 121B	-0.13542

Table S7. Occupancy and energy of Fe 3-d NAOs for $[\text{Fe}(\text{bpp})_2][\text{BF}_4]_2$.

NAO#	Atom	Label	Type	Occupancy	Energy
Low Spin					
25	Fe	dxy	Val(3d)	1.88932	-0.43675
28	Fe	dxz	Val(3d)	1.88931	-0.43675
31	Fe	dyz	Val(3d)	0.43071	-0.29722
34	Fe	dx ^{2+y²}	Val(3d)	0.84952	-0.33717
37	Fe	dz ²	Val(3d)	1.54918	-0.4021
High Spin α					
25	Fe	dxy	Val(3d)	0.98838	-0.55118
28	Fe	dxz	Val(3d)	0.98085	-0.49423
31	Fe	dyz	Val(3d)	0.99508	-0.54503
34	Fe	dx ^{2+y²}	Val(3d)	0.9936	-0.54461
37	Fe	dz ²	Val(3d)	0.98993	-0.53551
High Spin β					
25	Fe	dxy	Val(3d)	0.02251	-0.24382
28	Fe	dxz	Val(3d)	0.94037	-0.40063
31	Fe	dyz	Val(3d)	0.09387	-0.2458
34	Fe	dx ^{2+y²}	Val(3d)	0.08909	-0.24394
37	Fe	dz ²	Val(3d)	0.03183	-0.22075

Table S8. Orbital composition of MO-113A in HS state of $[\text{Fe}(\text{bpp})_2]\text{[BF}_4\text{]}_2$ (NAOs with composition less than 1% are omitted).

NAO#	Center	Label	Type	Composition
25	1(Fe)	dxy	Val(3d)	14.59%
68	2(N)	py	Val(2p)	2.46%
70	2(N)	pz	Val(2p)	2.32%
110	5(N)	py	Val(2p)	1.40%
124	6(N)	py	Val(2p)	1.38%
166	9(N)	py	Val(2p)	1.39%
180	10(N)	py	Val(2p)	2.57%
182	10(N)	pz	Val(2p)	2.20%
194	11(N)	py	Val(2p)	1.39%
292	18(C)	py	Val(2p)	3.23%
294	18(C)	pz	Val(2p)	3.29%
334	21(C)	py	Val(2p)	3.08%
336	21(C)	pz	Val(2p)	3.46%
432	28(C)	py	Val(2p)	3.22%
434	28(C)	pz	Val(2p)	3.29%
446	29(C)	py	Val(2p)	7.32%
448	29(C)	pz	Val(2p)	7.54%
460	30(C)	py	Val(2p)	3.08%
462	30(C)	pz	Val(2p)	3.46%
502	33(C)	py	Val(2p)	7.65%
504	33(C)	pz	Val(2p)	7.16%
Rydberg				0.23%

Table S9. Orbital composition of MO-120B in HS state of $[\text{Fe}(\text{bpp})_2]\text{[BF}_4\text{]}_2$ (NAOs with composition less than 0.3% are omitted).

NAO#	Center	Label	Type	Composition
28	1(Fe)	dxz	Val(3d)	87.35%
210	12(C)	pz	Val(2p)	0.44%
222	13(C)	py	Val(2p)	0.48%
236	14(C)	py	Val(2p)	0.47%
266	16(C)	pz	Val(2p)	0.45%
308	19(C)	pz	Val(2p)	0.44%
350	22(C)	pz	Val(2p)	0.43%
390	25(C)	py	Val(2p)	0.48%
446	29(C)	py	Val(2p)	0.34%
448	29(C)	pz	Val(2p)	0.47%
474	31(C)	py	Val(2p)	0.47%
502	33(C)	py	Val(2p)	0.36%
504	33(C)	pz	Val(2p)	0.45%
Rydberg				0.94%

Table S10 Orbital composition of MO-118 in LS state of $[\text{Fe}(\text{bpp})_2][\text{BF}_4]_2$ (NAOs with composition less than 1.0% are omitted).

NAO#	Center	Label	Type	Composition
82	3(N)	py	Val(2p)	2.53%
84	3(N)	pz	Val(2p)	2.58%
96	4(N)	py	Val(2p)	2.54%
98	4(N)	pz	Val(2p)	2.58%
138	7(N)	py	Val(2p)	2.55%
140	7(N)	pz	Val(2p)	2.51%
152	8(N)	py	Val(2p)	2.55%
154	8(N)	pz	Val(2p)	2.52%
208	12(C)	py	Val(2p)	2.33%
210	12(C)	pz	Val(2p)	2.38%
222	13(C)	py	Val(2p)	1.54%
224	13(C)	pz	Val(2p)	1.57%
236	14(C)	py	Val(2p)	1.55%
238	14(C)	pz	Val(2p)	1.53%
264	16(C)	py	Val(2p)	2.35%
266	16(C)	pz	Val(2p)	2.32%
278	17(C)	py	Val(2p)	1.61%
280	17(C)	pz	Val(2p)	1.64%
292	18(C)	py	Val(2p)	4.18%
294	18(C)	pz	Val(2p)	4.25%
306	19(C)	py	Val(2p)	2.35%
308	19(C)	pz	Val(2p)	2.32%
334	21(C)	py	Val(2p)	4.21%
336	21(C)	pz	Val(2p)	4.14%
348	22(C)	py	Val(2p)	2.34%
350	22(C)	pz	Val(2p)	2.37%
362	23(C)	py	Val(2p)	1.61%
364	23(C)	pz	Val(2p)	1.64%
390	25(C)	py	Val(2p)	1.54%
392	25(C)	pz	Val(2p)	1.57%
418	27(C)	py	Val(2p)	1.62%
420	27(C)	pz	Val(2p)	1.60%
432	28(C)	py	Val(2p)	4.18%
434	28(C)	pz	Val(2p)	4.25%
460	30(C)	py	Val(2p)	4.21%
462	30(C)	pz	Val(2p)	4.14%
474	31(C)	py	Val(2p)	1.55%
476	31(C)	pz	Val(2p)	1.53%
488	32(C)	py	Val(2p)	1.62%
490	32(C)	pz	Val(2p)	1.60%
Rydberg				0.38%

Table S11 Orbital composition of MO-119 in LS state $[\text{Fe}(\text{bpp})_2][\text{BF}_4]_2$ (NAOs with composition less than 1.0% are omitted).

NAO#	Center	Label	Type	Composition
82	3(N)	py	Val(2p)	2.46%
84	3(N)	pz	Val(2p)	2.51%
96	4(N)	py	Val(2p)	2.46%
98	4(N)	pz	Val(2p)	2.51%
138	7(N)	py	Val(2p)	2.53%
140	7(N)	pz	Val(2p)	2.49%
152	8(N)	py	Val(2p)	2.53%
154	8(N)	pz	Val(2p)	2.49%
208	12(C)	py	Val(2p)	1.88%
210	12(C)	pz	Val(2p)	1.91%
222	13(C)	py	Val(2p)	1.51%
224	13(C)	pz	Val(2p)	1.54%
236	14(C)	py	Val(2p)	1.55%
238	14(C)	pz	Val(2p)	1.53%
264	16(C)	py	Val(2p)	1.93%
266	16(C)	pz	Val(2p)	1.90%
278	17(C)	py	Val(2p)	2.08%
280	17(C)	pz	Val(2p)	2.11%
292	18(C)	py	Val(2p)	4.26%
294	18(C)	pz	Val(2p)	4.34%
306	19(C)	py	Val(2p)	1.93%
308	19(C)	pz	Val(2p)	1.90%
334	21(C)	py	Val(2p)	4.38%
336	21(C)	pz	Val(2p)	4.31%
348	22(C)	py	Val(2p)	1.88%
350	22(C)	pz	Val(2p)	1.91%
362	23(C)	py	Val(2p)	2.08%
364	23(C)	pz	Val(2p)	2.12%
390	25(C)	py	Val(2p)	1.51%
392	25(C)	pz	Val(2p)	1.54%
418	27(C)	py	Val(2p)	2.13%
420	27(C)	pz	Val(2p)	2.10%
432	28(C)	py	Val(2p)	4.26%
434	28(C)	pz	Val(2p)	4.34%
460	30(C)	py	Val(2p)	4.38%
462	30(C)	pz	Val(2p)	4.31%
474	31(C)	py	Val(2p)	1.56%
476	31(C)	pz	Val(2p)	1.53%
488	32(C)	py	Val(2p)	2.13%
490	32(C)	pz	Val(2p)	2.11%
Rydberg				0.39%

Table S12. Orbital composition of MO-123 in LS state of $[\text{Fe}(\text{bpp})_2][\text{BF}_4]_2$ (NAOs with composition less than 1.0% are omitted).

NAO#	Center	Label	Type	Composition
28	1(Fe)	dxz	Val(3d)	3.50%
68	2(N)	py	Val(2p)	2.72%
70	2(N)	pz	Val(2p)	2.51%
110	5(N)	py	Val(2p)	1.43%
180	10(N)	py	Val(2p)	7.31%
182	10(N)	pz	Val(2p)	7.28%
194	11(N)	py	Val(2p)	1.43%
208	12(C)	py	Val(2p)	1.95%
210	12(C)	pz	Val(2p)	1.63%
222	13(C)	py	Val(2p)	3.61%
224	13(C)	pz	Val(2p)	4.02%
236	14(C)	py	Val(2p)	1.21%
238	14(C)	pz	Val(2p)	1.53%
320	20(C)	py	Val(2p)	1.89%
322	20(C)	pz	Val(2p)	1.83%
348	22(C)	py	Val(2p)	1.95%
350	22(C)	pz	Val(2p)	1.62%
376	24(C)	py	Val(2p)	1.89%
378	24(C)	pz	Val(2p)	1.83%
390	25(C)	py	Val(2p)	3.60%
392	25(C)	pz	Val(2p)	4.02%
446	29(C)	py	Val(2p)	2.86%
448	29(C)	pz	Val(2p)	2.73%
474	31(C)	py	Val(2p)	1.21%
476	31(C)	pz	Val(2p)	1.53%
502	33(C)	py	Val(2p)	7.78%
504	33(C)	pz	Val(2p)	7.83%
Rydberg				1.93%

Table S13 Orbital composition of MO-124 in LS state of $[\text{Fe}(\text{bpp})_2][\text{BF}_4]_2$ (NAOs with composition less than 1.0% are omitted).

NAO#	Center	Label	Type	Composition
25	1(Fe)	dxy	Val(3d)	3.50%
68	2(N)	py	Val(2p)	7.28%
70	2(N)	pz	Val(2p)	7.32%
126	6(N)	pz	Val(2p)	1.44%
168	9(N)	pz	Val(2p)	1.44%
180	10(N)	py	Val(2p)	2.51%
182	10(N)	pz	Val(2p)	2.72%
222	13(C)	py	Val(2p)	1.53%
224	13(C)	pz	Val(2p)	1.21%
236	14(C)	py	Val(2p)	4.01%
238	14(C)	pz	Val(2p)	3.60%
250	15(C)	py	Val(2p)	1.83%
252	15(C)	pz	Val(2p)	1.90%
264	16(C)	py	Val(2p)	1.62%
266	16(C)	pz	Val(2p)	1.96%
306	19(C)	py	Val(2p)	1.62%
308	19(C)	pz	Val(2p)	1.95%
390	25(C)	py	Val(2p)	1.53%
392	25(C)	pz	Val(2p)	1.21%
404	26(C)	py	Val(2p)	1.83%
406	26(C)	pz	Val(2p)	1.90%
446	29(C)	py	Val(2p)	7.83%
448	29(C)	pz	Val(2p)	7.79%
474	31(C)	py	Val(2p)	4.02%
476	31(C)	pz	Val(2p)	3.61%
502	33(C)	py	Val(2p)	2.73%
504	33(C)	pz	Val(2p)	2.87%
Rydberg				1.92%

Table S14 Orbital composition of MO-126 in LS state of $[\text{Fe}(\text{bpp})_2][\text{BF}_4]_2$ (NAOs with composition less than 1.0% are omitted)

NAO#	Center	Label	Type	Composition
110	5(N)	py	Val(2p)	1.24%
112	5(N)	pz	Val(2p)	1.26%
124	6(N)	py	Val(2p)	1.26%
126	6(N)	pz	Val(2p)	1.24%
166	9(N)	py	Val(2p)	1.25%
168	9(N)	pz	Val(2p)	1.24%
194	11(N)	py	Val(2p)	1.23%
196	11(N)	pz	Val(2p)	1.26%
208	12(C)	py	Val(2p)	1.06%
210	12(C)	pz	Val(2p)	1.08%
222	13(C)	py	Val(2p)	2.79%
224	13(C)	pz	Val(2p)	2.84%
236	14(C)	py	Val(2p)	2.84%
238	14(C)	pz	Val(2p)	2.79%
250	15(C)	py	Val(2p)	1.88%
252	15(C)	pz	Val(2p)	1.86%
264	16(C)	py	Val(2p)	1.07%
266	16(C)	pz	Val(2p)	1.06%
292	18(C)	py	Val(2p)	4.43%
294	18(C)	pz	Val(2p)	4.51%
306	19(C)	py	Val(2p)	1.07%
308	19(C)	pz	Val(2p)	1.06%
320	20(C)	py	Val(2p)	1.85%
322	20(C)	pz	Val(2p)	1.89%
334	21(C)	py	Val(2p)	4.50%
336	21(C)	pz	Val(2p)	4.42%
348	22(C)	py	Val(2p)	1.06%
350	22(C)	pz	Val(2p)	1.08%
376	24(C)	py	Val(2p)	1.86%
378	24(C)	pz	Val(2p)	1.89%
390	25(C)	py	Val(2p)	2.80%
392	25(C)	pz	Val(2p)	2.85%
404	26(C)	py	Val(2p)	1.88%
406	26(C)	pz	Val(2p)	1.86%
432	28(C)	py	Val(2p)	4.43%
434	28(C)	pz	Val(2p)	4.51%
460	30(C)	py	Val(2p)	4.50%
462	30(C)	pz	Val(2p)	4.42%
474	31(C)	py	Val(2p)	2.84%
476	31(C)	pz	Val(2p)	2.79%
Rydberg				2.55%

Table S15 Orbital composition of MO-129 in LS state of $[\text{Fe}(\text{bpp})_2][\text{BF}_4]_2$ (NAOs with composition less than 1.0% are omitted)

NAO#	Center	Label	Type	Composition
82	3(N)	py	Val(2p)	2.47%
84	3(N)	pz	Val(2p)	2.51%
96	4(N)	py	Val(2p)	2.47%
98	4(N)	pz	Val(2p)	2.51%
110	5(N)	py	Val(2p)	2.55%
112	5(N)	pz	Val(2p)	2.94%
124	6(N)	py	Val(2p)	1.34%
126	6(N)	pz	Val(2p)	1.69%
138	7(N)	py	Val(2p)	1.38%
140	7(N)	pz	Val(2p)	1.35%
152	8(N)	py	Val(2p)	1.38%
154	8(N)	pz	Val(2p)	1.35%
166	9(N)	py	Val(2p)	1.34%
168	9(N)	pz	Val(2p)	1.69%
194	11(N)	py	Val(2p)	2.53%
196	11(N)	pz	Val(2p)	2.97%
208	12(C)	py	Val(2p)	2.00%
210	12(C)	pz	Val(2p)	2.15%
250	15(C)	py	Val(2p)	1.67%
252	15(C)	pz	Val(2p)	1.72%
264	16(C)	py	Val(2p)	1.09%
266	16(C)	pz	Val(2p)	1.19%
292	18(C)	py	Val(2p)	1.59%
294	18(C)	pz	Val(2p)	1.62%
306	19(C)	py	Val(2p)	1.09%
308	19(C)	pz	Val(2p)	1.19%
320	20(C)	py	Val(2p)	3.02%
322	20(C)	pz	Val(2p)	3.16%
348	22(C)	py	Val(2p)	2.00%
350	22(C)	pz	Val(2p)	2.14%
376	24(C)	py	Val(2p)	3.03%
378	24(C)	pz	Val(2p)	3.15%
404	26(C)	py	Val(2p)	1.67%
406	26(C)	pz	Val(2p)	1.72%
432	28(C)	py	Val(2p)	1.59%
434	28(C)	pz	Val(2p)	1.62%
446	29(C)	py	Val(2p)	3.04%
448	29(C)	pz	Val(2p)	2.95%
502	33(C)	py	Val(2p)	5.42%
504	33(C)	pz	Val(2p)	5.48%
Rydberg				3.33%

Table S16 Orbital composition of MO-122A in HS state of $[\text{Fe}(\text{bpp})_2][\text{BF}_4]_2$ (NAOs with composition less than 1.0% are omitted)

NAO#	Center	Label	Type	Composition
82	3(N)	py	Val(2p)	2.77%
84	3(N)	pz	Val(2p)	2.52%
96	4(N)	py	Val(2p)	2.77%
98	4(N)	pz	Val(2p)	2.51%
138	7(N)	py	Val(2p)	2.48%
140	7(N)	pz	Val(2p)	2.47%
152	8(N)	py	Val(2p)	2.48%
154	8(N)	pz	Val(2p)	2.46%
208	12(C)	py	Val(2p)	2.29%
210	12(C)	pz	Val(2p)	2.01%
222	13(C)	py	Val(2p)	1.66%
224	13(C)	pz	Val(2p)	1.63%
236	14(C)	py	Val(2p)	1.48%
238	14(C)	pz	Val(2p)	1.60%
264	16(C)	py	Val(2p)	2.06%
266	16(C)	pz	Val(2p)	1.98%
278	17(C)	py	Val(2p)	1.97%
280	17(C)	pz	Val(2p)	1.77%
292	18(C)	py	Val(2p)	4.58%
294	18(C)	pz	Val(2p)	4.43%
306	19(C)	py	Val(2p)	2.06%
308	19(C)	pz	Val(2p)	1.97%
334	21(C)	py	Val(2p)	4.09%
336	21(C)	pz	Val(2p)	4.35%
348	22(C)	py	Val(2p)	2.29%
350	22(C)	pz	Val(2p)	2.01%
362	23(C)	py	Val(2p)	1.98%
364	23(C)	pz	Val(2p)	1.77%
390	25(C)	py	Val(2p)	1.66%
392	25(C)	pz	Val(2p)	1.63%
418	27(C)	py	Val(2p)	1.76%
420	27(C)	pz	Val(2p)	1.74%
432	28(C)	py	Val(2p)	4.58%
434	28(C)	pz	Val(2p)	4.43%
460	30(C)	py	Val(2p)	4.09%
462	30(C)	pz	Val(2p)	4.35%
474	31(C)	py	Val(2p)	1.48%
476	31(C)	pz	Val(2p)	1.60%
488	32(C)	py	Val(2p)	1.76%
490	32(C)	pz	Val(2p)	1.73%
		Rydberg		0.40%

Table S17 Orbital composition of MO-123A in HS state of $[\text{Fe}(\text{bpp})_2][\text{BF}_4]_2$ (NAOs with composition less than 1.0% are omitted)

NAO#	Center	Label	Type	Composition
82	3(N)	py	Val(2p)	2.59%
84	3(N)	pz	Val(2p)	2.39%
96	4(N)	py	Val(2p)	2.59%
98	4(N)	pz	Val(2p)	2.38%
138	7(N)	py	Val(2p)	2.64%
140	7(N)	pz	Val(2p)	2.68%
152	8(N)	py	Val(2p)	2.64%
154	8(N)	pz	Val(2p)	2.67%
208	12(C)	py	Val(2p)	2.02%
210	12(C)	pz	Val(2p)	1.86%
222	13(C)	py	Val(2p)	1.58%
224	13(C)	pz	Val(2p)	1.44%
236	14(C)	py	Val(2p)	1.61%
238	14(C)	pz	Val(2p)	1.62%
264	16(C)	py	Val(2p)	2.07%
266	16(C)	pz	Val(2p)	2.09%
278	17(C)	py	Val(2p)	2.02%
280	17(C)	pz	Val(2p)	1.70%
292	18(C)	py	Val(2p)	4.19%
294	18(C)	pz	Val(2p)	4.10%
306	19(C)	py	Val(2p)	2.07%
308	19(C)	pz	Val(2p)	2.08%
334	21(C)	py	Val(2p)	4.28%
336	21(C)	pz	Val(2p)	4.58%
348	22(C)	py	Val(2p)	2.02%
350	22(C)	pz	Val(2p)	1.86%
362	23(C)	py	Val(2p)	2.03%
364	23(C)	pz	Val(2p)	1.71%
390	25(C)	py	Val(2p)	1.58%
392	25(C)	pz	Val(2p)	1.44%
418	27(C)	py	Val(2p)	2.07%
420	27(C)	pz	Val(2p)	1.92%
432	28(C)	py	Val(2p)	4.20%
434	28(C)	pz	Val(2p)	4.10%
460	30(C)	py	Val(2p)	4.27%
462	30(C)	pz	Val(2p)	4.59%
474	31(C)	py	Val(2p)	1.61%
476	31(C)	pz	Val(2p)	1.62%
488	32(C)	py	Val(2p)	2.06%
490	32(C)	pz	Val(2p)	1.90%
Rydberg				0.39%

Table S18 Orbital composition of MO-125A in HS state of $[\text{Fe}(\text{bpp})_2][\text{BF}_4]_2$ (NAOs with composition less than 1.0% are omitted)

NAO#	Center	Label	Type	Composition
68	2(N)	py	Val(2p)	4.87%
70	2(N)	pz	Val(2p)	5.14%
180	10(N)	py	Val(2p)	5.05%
182	10(N)	pz	Val(2p)	4.87%
208	12(C)	py	Val(2p)	1.25%
210	12(C)	pz	Val(2p)	1.38%
222	13(C)	py	Val(2p)	2.83%
224	13(C)	pz	Val(2p)	2.62%
236	14(C)	py	Val(2p)	2.73%
238	14(C)	pz	Val(2p)	2.78%
250	15(C)	py	Val(2p)	1.31%
252	15(C)	pz	Val(2p)	1.37%
264	16(C)	py	Val(2p)	1.20%
266	16(C)	pz	Val(2p)	1.45%
306	19(C)	py	Val(2p)	1.20%
308	19(C)	pz	Val(2p)	1.45%
320	20(C)	py	Val(2p)	1.36%
322	20(C)	pz	Val(2p)	1.30%
348	22(C)	py	Val(2p)	1.25%
350	22(C)	pz	Val(2p)	1.38%
376	24(C)	py	Val(2p)	1.37%
378	24(C)	pz	Val(2p)	1.30%
390	25(C)	py	Val(2p)	2.83%
392	25(C)	pz	Val(2p)	2.63%
404	26(C)	py	Val(2p)	1.32%
406	26(C)	pz	Val(2p)	1.37%
446	29(C)	py	Val(2p)	5.34%
448	29(C)	pz	Val(2p)	5.65%
474	31(C)	py	Val(2p)	2.72%
476	31(C)	pz	Val(2p)	2.78%
502	33(C)	py	Val(2p)	5.55%
504	33(C)	pz	Val(2p)	5.35%
Rydberg				2.12%

Table S19 Orbital composition of MO-126A in HS state of $[\text{Fe}(\text{bpp})_2][\text{BF}_4]_2$ (NAOs with composition less than 1.0% are omitted)

NAO#	Center	Label	Type	Composition
28	1(Fe)	dxz	Val(3d)	1.02%
68	2(N)	py	Val(2p)	4.89%
70	2(N)	pz	Val(2p)	5.09%
110	5(N)	py	Val(2p)	1.03%
180	10(N)	py	Val(2p)	5.17%
182	10(N)	pz	Val(2p)	4.89%
194	11(N)	py	Val(2p)	1.02%
208	12(C)	py	Val(2p)	1.50%
210	12(C)	pz	Val(2p)	1.05%
222	13(C)	py	Val(2p)	2.68%
224	13(C)	pz	Val(2p)	2.76%
236	14(C)	py	Val(2p)	2.54%
238	14(C)	pz	Val(2p)	2.88%
250	15(C)	py	Val(2p)	1.37%
252	15(C)	pz	Val(2p)	1.22%
264	16(C)	py	Val(2p)	1.43%
266	16(C)	pz	Val(2p)	1.10%
306	19(C)	py	Val(2p)	1.44%
308	19(C)	pz	Val(2p)	1.11%
320	20(C)	py	Val(2p)	1.44%
322	20(C)	pz	Val(2p)	1.18%
348	22(C)	py	Val(2p)	1.51%
350	22(C)	pz	Val(2p)	1.06%
376	24(C)	py	Val(2p)	1.46%
378	24(C)	pz	Val(2p)	1.18%
390	25(C)	py	Val(2p)	2.69%
392	25(C)	pz	Val(2p)	2.77%
404	26(C)	py	Val(2p)	1.39%
406	26(C)	pz	Val(2p)	1.23%
446	29(C)	py	Val(2p)	5.33%
448	29(C)	pz	Val(2p)	5.62%
474	31(C)	py	Val(2p)	2.53%
476	31(C)	pz	Val(2p)	2.86%
502	33(C)	py	Val(2p)	5.64%
504	33(C)	pz	Val(2p)	5.41%
Rydberg				2.07%

Table S20 Orbital composition of MO-127A in HS state of $[\text{Fe}(\text{bpp})_2][\text{BF}_4]_2$ (NAOs with composition less than 1.0% are omitted)

NAO#	Center	Label	Type	Composition
110	5(N)	py	Val(2p)	1.41%
112	5(N)	pz	Val(2p)	1.25%
124	6(N)	py	Val(2p)	1.35%
126	6(N)	pz	Val(2p)	1.32%
166	9(N)	py	Val(2p)	1.34%
168	9(N)	pz	Val(2p)	1.31%
194	11(N)	py	Val(2p)	1.41%
196	11(N)	pz	Val(2p)	1.26%
208	12(C)	py	Val(2p)	1.40%
210	12(C)	pz	Val(2p)	1.27%
222	13(C)	py	Val(2p)	2.61%
224	13(C)	pz	Val(2p)	2.53%
236	14(C)	py	Val(2p)	2.47%
238	14(C)	pz	Val(2p)	2.63%
250	15(C)	py	Val(2p)	2.11%
252	15(C)	pz	Val(2p)	2.01%
264	16(C)	py	Val(2p)	1.34%
266	16(C)	pz	Val(2p)	1.32%
292	18(C)	py	Val(2p)	4.30%
294	18(C)	pz	Val(2p)	4.17%
306	19(C)	py	Val(2p)	1.34%
308	19(C)	pz	Val(2p)	1.32%
320	20(C)	py	Val(2p)	2.21%
322	20(C)	pz	Val(2p)	1.92%
334	21(C)	py	Val(2p)	4.09%
336	21(C)	pz	Val(2p)	4.36%
348	22(C)	py	Val(2p)	1.40%
350	22(C)	pz	Val(2p)	1.26%
376	24(C)	py	Val(2p)	2.20%
378	24(C)	pz	Val(2p)	1.90%
390	25(C)	py	Val(2p)	2.59%
392	25(C)	pz	Val(2p)	2.52%
404	26(C)	py	Val(2p)	2.11%
406	26(C)	pz	Val(2p)	1.99%
432	28(C)	py	Val(2p)	4.28%
434	28(C)	pz	Val(2p)	4.17%
460	30(C)	py	Val(2p)	4.08%
462	30(C)	pz	Val(2p)	4.36%
474	31(C)	py	Val(2p)	2.48%
476	31(C)	pz	Val(2p)	2.65%
Rydberg				2.42%

Table S21 Orbital composition of MO-128A in HS state of $[\text{Fe}(\text{bpp})_2][\text{BF}_4]_2$ (NAOs with composition less than 1.0% are omitted)

NAO#	Center	Label	Type	Composition
110	5(N)	py	Val(2p)	1.34%
112	5(N)	pz	Val(2p)	1.20%
124	6(N)	py	Val(2p)	1.28%
126	6(N)	pz	Val(2p)	1.26%
166	9(N)	py	Val(2p)	1.28%
168	9(N)	pz	Val(2p)	1.26%
194	11(N)	py	Val(2p)	1.34%
196	11(N)	pz	Val(2p)	1.20%
208	12(C)	py	Val(2p)	1.15%
210	12(C)	pz	Val(2p)	1.04%
222	13(C)	py	Val(2p)	2.88%
224	13(C)	pz	Val(2p)	2.76%
236	14(C)	py	Val(2p)	2.75%
238	14(C)	pz	Val(2p)	2.89%
250	15(C)	py	Val(2p)	1.92%
252	15(C)	pz	Val(2p)	1.82%
264	16(C)	py	Val(2p)	1.10%
266	16(C)	pz	Val(2p)	1.09%
292	18(C)	py	Val(2p)	4.50%
294	18(C)	pz	Val(2p)	4.38%
306	19(C)	py	Val(2p)	1.10%
308	19(C)	pz	Val(2p)	1.09%
320	20(C)	py	Val(2p)	2.01%
322	20(C)	pz	Val(2p)	1.73%
334	21(C)	py	Val(2p)	4.30%
336	21(C)	pz	Val(2p)	4.60%
348	22(C)	py	Val(2p)	1.15%
350	22(C)	pz	Val(2p)	1.04%
376	24(C)	py	Val(2p)	2.01%
378	24(C)	pz	Val(2p)	1.73%
390	25(C)	py	Val(2p)	2.87%
392	25(C)	pz	Val(2p)	2.76%
404	26(C)	py	Val(2p)	1.93%
406	26(C)	pz	Val(2p)	1.82%
432	28(C)	py	Val(2p)	4.49%
434	28(C)	pz	Val(2p)	4.38%
460	30(C)	py	Val(2p)	4.29%
462	30(C)	pz	Val(2p)	4.60%
474	31(C)	py	Val(2p)	2.75%
476	31(C)	pz	Val(2p)	2.90%
Rydberg				2.50%

Table S22 Orbital composition of MO-117B in HS state of $[\text{Fe}(\text{bpp})_2][\text{BF}_4]_2$ (NAOs with composition less than 1.0% are omitted)

NAO#	Center	Label	Type	Composition
68	2(N)	py	Val(2p)	1.19%
70	2(N)	pz	Val(2p)	1.34%
82	3(N)	py	Val(2p)	1.14%
96	4(N)	py	Val(2p)	1.15%
110	5(N)	py	Val(2p)	1.73%
112	5(N)	pz	Val(2p)	2.34%
124	6(N)	py	Val(2p)	1.79%
126	6(N)	pz	Val(2p)	2.63%
138	7(N)	py	Val(2p)	1.15%
140	7(N)	pz	Val(2p)	1.05%
152	8(N)	py	Val(2p)	1.16%
154	8(N)	pz	Val(2p)	1.06%
166	9(N)	py	Val(2p)	1.73%
168	9(N)	pz	Val(2p)	2.53%
180	10(N)	py	Val(2p)	1.19%
182	10(N)	pz	Val(2p)	1.22%
194	11(N)	py	Val(2p)	1.79%
196	11(N)	pz	Val(2p)	2.44%
250	15(C)	py	Val(2p)	2.99%
252	15(C)	pz	Val(2p)	2.71%
278	17(C)	py	Val(2p)	5.56%
280	17(C)	pz	Val(2p)	4.65%
320	20(C)	py	Val(2p)	2.99%
322	20(C)	pz	Val(2p)	2.46%
362	23(C)	py	Val(2p)	5.65%
364	23(C)	pz	Val(2p)	4.74%
376	24(C)	py	Val(2p)	2.88%
378	24(C)	pz	Val(2p)	2.37%
404	26(C)	py	Val(2p)	2.89%
406	26(C)	pz	Val(2p)	2.61%
418	27(C)	py	Val(2p)	5.67%
420	27(C)	pz	Val(2p)	5.23%
488	32(C)	py	Val(2p)	5.59%
490	32(C)	pz	Val(2p)	5.13%
Rydberg				0.29%

Table S23 Orbital composition of MO-118B in HS state of $[\text{Fe}(\text{bpp})_2][\text{BF}_4]_2$ (NAOs with composition less than 1.0% are omitted)

NAO#	Center	Label	Type	Composition
82	3(N)	py	Val(2p)	2.92%
84	3(N)	pz	Val(2p)	2.64%
96	4(N)	py	Val(2p)	2.91%
98	4(N)	pz	Val(2p)	2.63%
138	7(N)	py	Val(2p)	2.37%
140	7(N)	pz	Val(2p)	2.34%
152	8(N)	py	Val(2p)	2.36%
154	8(N)	pz	Val(2p)	2.33%
208	12(C)	py	Val(2p)	2.40%
210	12(C)	pz	Val(2p)	2.13%
222	13(C)	py	Val(2p)	1.74%
224	13(C)	pz	Val(2p)	1.70%
236	14(C)	py	Val(2p)	1.41%
238	14(C)	pz	Val(2p)	1.51%
264	16(C)	py	Val(2p)	1.94%
266	16(C)	pz	Val(2p)	1.90%
278	17(C)	py	Val(2p)	2.10%
280	17(C)	pz	Val(2p)	1.85%
292	18(C)	py	Val(2p)	4.77%
294	18(C)	pz	Val(2p)	4.62%
306	19(C)	py	Val(2p)	1.94%
308	19(C)	pz	Val(2p)	1.89%
334	21(C)	py	Val(2p)	3.86%
336	21(C)	pz	Val(2p)	4.11%
348	22(C)	py	Val(2p)	2.39%
350	22(C)	pz	Val(2p)	2.12%
362	23(C)	py	Val(2p)	2.10%
364	23(C)	pz	Val(2p)	1.86%
390	25(C)	py	Val(2p)	1.75%
392	25(C)	pz	Val(2p)	1.70%
418	27(C)	py	Val(2p)	1.70%
420	27(C)	pz	Val(2p)	1.65%
432	28(C)	py	Val(2p)	4.77%
434	28(C)	pz	Val(2p)	4.62%
460	30(C)	py	Val(2p)	3.86%
462	30(C)	pz	Val(2p)	4.11%
474	31(C)	py	Val(2p)	1.41%
476	31(C)	pz	Val(2p)	1.51%
488	32(C)	py	Val(2p)	1.70%
490	32(C)	pz	Val(2p)	1.64%
Rydberg				0.40%

Table S24 Orbital composition of MO-119B in HS state of $[\text{Fe}(\text{bpp})_2][\text{BF}_4]_2$ (NAOs with composition less than 1.0% are omitted)

NAO#	Center	Label	Type	Composition
82	3(N)	py	Val(2p)	2.50%
84	3(N)	pz	Val(2p)	2.26%
96	4(N)	py	Val(2p)	2.49%
98	4(N)	pz	Val(2p)	2.25%
138	7(N)	py	Val(2p)	2.81%
140	7(N)	pz	Val(2p)	2.79%
152	8(N)	py	Val(2p)	2.81%
154	8(N)	pz	Val(2p)	2.78%
208	12(C)	py	Val(2p)	2.03%
210	12(C)	pz	Val(2p)	1.80%
222	13(C)	py	Val(2p)	1.47%
224	13(C)	pz	Val(2p)	1.43%
236	14(C)	py	Val(2p)	1.65%
238	14(C)	pz	Val(2p)	1.77%
264	16(C)	py	Val(2p)	2.29%
266	16(C)	pz	Val(2p)	2.24%
278	17(C)	py	Val(2p)	1.81%
280	17(C)	pz	Val(2p)	1.60%
292	18(C)	py	Val(2p)	4.00%
294	18(C)	pz	Val(2p)	3.87%
306	19(C)	py	Val(2p)	2.29%
308	19(C)	pz	Val(2p)	2.23%
334	21(C)	py	Val(2p)	4.50%
336	21(C)	pz	Val(2p)	4.79%
348	22(C)	py	Val(2p)	2.03%
350	22(C)	pz	Val(2p)	1.80%
362	23(C)	py	Val(2p)	1.81%
364	23(C)	pz	Val(2p)	1.61%
390	25(C)	py	Val(2p)	1.47%
392	25(C)	pz	Val(2p)	1.43%
418	27(C)	py	Val(2p)	2.04%
420	27(C)	pz	Val(2p)	1.98%
432	28(C)	py	Val(2p)	4.00%
434	28(C)	pz	Val(2p)	3.87%
460	30(C)	py	Val(2p)	4.50%
462	30(C)	pz	Val(2p)	4.79%
474	31(C)	py	Val(2p)	1.65%
476	31(C)	pz	Val(2p)	1.77%
488	32(C)	py	Val(2p)	2.04%
490	32(C)	pz	Val(2p)	1.97%
Rydberg				0.38%

Table S25 Orbital composition of MO-121B in HS state of $[\text{Fe}(\text{bpp})_2][\text{BF}_4]_2$ (NAOs with composition less than 0.3% are omitted).

NAO#	Center	Label	Type	Composition
25	1(Fe)	dxy	Val(3d)	24.31%
68	2(N)	py	Val(2p)	3.45%
70	2(N)	pz	Val(2p)	3.04%
110	5(N)	py	Val(2p)	0.66%
112	5(N)	pz	Val(2p)	0.35%
124	6(N)	py	Val(2p)	0.64%
126	6(N)	pz	Val(2p)	0.38%
166	9(N)	py	Val(2p)	0.64%
168	9(N)	pz	Val(2p)	0.38%
180	10(N)	py	Val(2p)	3.59%
182	10(N)	pz	Val(2p)	2.87%
194	11(N)	py	Val(2p)	0.66%
196	11(N)	pz	Val(2p)	0.36%
208	12(C)	py	Val(2p)	1.30%
210	12(C)	pz	Val(2p)	0.99%
222	13(C)	py	Val(2p)	2.09%
224	13(C)	pz	Val(2p)	2.57%
236	14(C)	py	Val(2p)	1.99%
238	14(C)	pz	Val(2p)	2.69%
250	15(C)	py	Val(2p)	1.02%
252	15(C)	pz	Val(2p)	1.06%
264	16(C)	py	Val(2p)	1.25%
266	16(C)	pz	Val(2p)	1.05%
306	19(C)	py	Val(2p)	1.25%
308	19(C)	pz	Val(2p)	1.04%
320	20(C)	py	Val(2p)	1.06%
322	20(C)	pz	Val(2p)	1.01%
348	22(C)	py	Val(2p)	1.29%
350	22(C)	pz	Val(2p)	0.98%
376	24(C)	py	Val(2p)	1.06%
378	24(C)	pz	Val(2p)	1.00%
390	25(C)	py	Val(2p)	2.09%
392	25(C)	pz	Val(2p)	2.57%
404	26(C)	py	Val(2p)	1.02%
406	26(C)	pz	Val(2p)	1.05%
446	29(C)	py	Val(2p)	4.08%
448	29(C)	pz	Val(2p)	4.08%
474	31(C)	py	Val(2p)	1.99%
476	31(C)	pz	Val(2p)	2.70%
502	33(C)	py	Val(2p)	4.25%
504	33(C)	pz	Val(2p)	3.87%
Rydberg				2.36%

Table S26 Orbital composition of MO-123B in HS state of $[\text{Fe}(\text{bpp})_2][\text{BF}_4]_2$ (NAOs with composition less than 0.3% are omitted).

NAO#	Center	Label	Type	Composition
28	1(Fe)	dxz	Val(3d)	3.93%
68	2(N)	py	Val(2p)	5.02%
70	2(N)	pz	Val(2p)	5.06%
110	5(N)	py	Val(2p)	1.01%
124	6(N)	py	Val(2p)	1.02%
180	10(N)	py	Val(2p)	5.29%
182	10(N)	pz	Val(2p)	4.86%
194	11(N)	py	Val(2p)	1.06%
208	12(C)	py	Val(2p)	1.43%
222	13(C)	py	Val(2p)	2.51%
224	13(C)	pz	Val(2p)	2.72%
236	14(C)	py	Val(2p)	2.28%
238	14(C)	pz	Val(2p)	2.72%
250	15(C)	py	Val(2p)	1.33%
252	15(C)	pz	Val(2p)	1.20%
264	16(C)	py	Val(2p)	1.37%
306	19(C)	py	Val(2p)	1.30%
320	20(C)	py	Val(2p)	1.39%
322	20(C)	pz	Val(2p)	1.15%
348	22(C)	py	Val(2p)	1.36%
376	24(C)	py	Val(2p)	1.32%
378	24(C)	pz	Val(2p)	1.08%
390	25(C)	py	Val(2p)	2.41%
392	25(C)	pz	Val(2p)	2.62%
404	26(C)	py	Val(2p)	1.25%
406	26(C)	pz	Val(2p)	1.12%
446	29(C)	py	Val(2p)	5.28%
448	29(C)	pz	Val(2p)	5.51%
474	31(C)	py	Val(2p)	2.37%
476	31(C)	pz	Val(2p)	2.83%
502	33(C)	py	Val(2p)	5.57%
504	33(C)	pz	Val(2p)	5.29%
Rydberg				1.94%

Table S27 Orbital composition of MO-124B in HS state of $[\text{Fe}(\text{bpp})_2][\text{BF}_4]_2$ (NAOs with composition less than 0.3% are omitted).

NAO#	Center	Label	Type	Composition
110	5(N)	py	Val(2p)	1.25%
112	5(N)	pz	Val(2p)	1.27%
124	6(N)	py	Val(2p)	1.19%
126	6(N)	pz	Val(2p)	1.32%
166	9(N)	py	Val(2p)	1.20%
168	9(N)	pz	Val(2p)	1.33%
194	11(N)	py	Val(2p)	1.25%
196	11(N)	pz	Val(2p)	1.26%
208	12(C)	py	Val(2p)	1.10%
210	12(C)	pz	Val(2p)	1.03%
222	13(C)	py	Val(2p)	2.90%
224	13(C)	pz	Val(2p)	2.75%
236	14(C)	py	Val(2p)	2.78%
238	14(C)	pz	Val(2p)	2.90%
250	15(C)	py	Val(2p)	1.88%
252	15(C)	pz	Val(2p)	1.82%
264	16(C)	py	Val(2p)	1.06%
266	16(C)	pz	Val(2p)	1.08%
292	18(C)	py	Val(2p)	4.53%
294	18(C)	pz	Val(2p)	4.41%
306	19(C)	py	Val(2p)	1.06%
308	19(C)	pz	Val(2p)	1.08%
320	20(C)	py	Val(2p)	1.96%
322	20(C)	pz	Val(2p)	1.73%
334	21(C)	py	Val(2p)	4.33%
336	21(C)	pz	Val(2p)	4.63%
348	22(C)	py	Val(2p)	1.11%
350	22(C)	pz	Val(2p)	1.03%
376	24(C)	py	Val(2p)	1.97%
378	24(C)	pz	Val(2p)	1.73%
390	25(C)	py	Val(2p)	2.91%
392	25(C)	pz	Val(2p)	2.76%
404	26(C)	py	Val(2p)	1.89%
406	26(C)	pz	Val(2p)	1.82%
432	28(C)	py	Val(2p)	4.53%
434	28(C)	pz	Val(2p)	4.41%
460	30(C)	py	Val(2p)	4.33%
462	30(C)	pz	Val(2p)	4.64%
474	31(C)	py	Val(2p)	2.77%
476	31(C)	pz	Val(2p)	2.89%
Rydberg				2.52%

Table S28 Orbital composition of MO-126B in HS state of $[\text{Fe}(\text{bpp})_2][\text{BF}_4]_2$ (NAOs with composition less than 0.3% are omitted).

NAO#	Center	Label	Type	Composition
25	1(Fe)	dxy	Val(3d)	67.86%
68	2(N)	py	Val(2p)	1.26%
70	2(N)	pz	Val(2p)	2.28%
112	5(N)	pz	Val(2p)	0.50%
126	6(N)	pz	Val(2p)	0.50%
168	9(N)	pz	Val(2p)	0.51%
180	10(N)	py	Val(2p)	1.33%
182	10(N)	pz	Val(2p)	2.18%
196	11(N)	pz	Val(2p)	0.49%
210	12(C)	pz	Val(2p)	0.32%
222	13(C)	py	Val(2p)	0.80%
236	14(C)	py	Val(2p)	0.78%
250	15(C)	py	Val(2p)	0.34%
266	16(C)	pz	Val(2p)	0.33%
292	18(C)	py	Val(2p)	0.36%
294	18(C)	pz	Val(2p)	0.32%
308	19(C)	pz	Val(2p)	0.33%
320	20(C)	py	Val(2p)	0.35%
334	21(C)	py	Val(2p)	0.34%
336	21(C)	pz	Val(2p)	0.34%
350	22(C)	pz	Val(2p)	0.32%
376	24(C)	py	Val(2p)	0.35%
390	25(C)	py	Val(2p)	0.80%
404	26(C)	py	Val(2p)	0.33%
432	28(C)	py	Val(2p)	0.35%
434	28(C)	pz	Val(2p)	0.31%
446	29(C)	py	Val(2p)	1.51%
448	29(C)	pz	Val(2p)	1.89%
460	30(C)	py	Val(2p)	0.34%
462	30(C)	pz	Val(2p)	0.33%
474	31(C)	py	Val(2p)	0.79%
502	33(C)	py	Val(2p)	1.58%
504	33(C)	pz	Val(2p)	1.80%
Rydberg				1.68%